Catalysis Today 158 (2010) 361–369

Contents lists available at ScienceDirect

Catalysis Today

journal homepage: www.elsevier.com/locate/cattod

Catalytic oxidation of NO over TiO_2 supported platinum clusters. II: Mechanism study by in situ FTIR spectra

Landong Li[a,b], Qun shen[a], Jie Cheng[a], Zhengping Hao[a,*]

[a] *Research Center for Eco-Environmental Sciences, Chinese Academy of Sciences, Beijing 100085, PR China*
[b] *Institute of New Catalytic Materials Science, College of Chemistry, Nankai University, Tianjin 300071, PR China*

ARTICLE INFO

Article history:
Available online 31 May 2010

Keywords:
Pt/TiO_2
NO oxidation
SO_2
In situ FTIR

ABSTRACT

The surface species formed during NO oxidation in the absence/presence of SO_2 over Pt/TiO_2 catalyst prepared by photo-deposition are investigated by in situ FTIR spectroscopy. During the adsorption of $NO–O_2$, predominant various nitrates are formed on the surface of TiO_2. The addition of SO_2 to $NO–O_2$ greatly suppresses the formation of surface nitrates and also changes the types of nitrates formed. The decomposition of surface nitrates on Pt/TiO_2 is observed at elevated temperature of *ca.* 250 °C and the decomposition temperature is retarded to *ca.* 350 °C with the addition of SO_2 during $NO–O_2$ adsorption. The direct oxidation of gaseous NO to NO_2 is proposed as the main pathway for NO_2 formation and the decomposition of surface nitrates at elevated temperatures plays a negative role on NO oxidation.

1. Introduction

Nitrogen oxides (NO*x*) are major air pollutions that greatly contribute to the formation of photochemical smog and acid rain. Various techniques, *e.g.* selective catalytic reduction of NO*x* (SCR) [1] and NO*x* storage-reduction (NSR) [2], have been developed for the elimination of nitrogen oxides from anthropogenic sources. It is generally accepted that NO_2 plays a key role for these techniques. It is also known that most nitrogen oxides exist in the form of NO (>90%). So, the oxidation of NO to NO_2 is regarded as a very important reaction and eligible catalysts for NO oxidation are being researched.

Precious metal platinum is the primary choice of active component for NO oxidation and supported platinum catalysts are extensively investigated. Especially, the mechanism aspect for NO oxidation on platinum catalysts has drawn much attention. In the early work of Xue et al. [3], the authors proposed a process that NO first adsorbed on support, migrated to Pt sites and then oxidized to NO_2. Thus the strength of bond between Pt and support was regarded as a key factor controlling the NO oxidation activity on supported Pt catalysts. A different opinion of Olsson et al. [4] suggested an Eley–Rideal model for NO oxidation over Pt/Al_2O_3 and the rate-determination step was recognized as $Pt–O + NO\ (g) \rightarrow Pt–NO_2$. They further improved this model to a combination of Eley–Rideal and Langmuir–Hinshelwood ($Pt–O + Pt–NO \rightarrow Pt + Pt–NO_2$) mechanism [5]. In a recent study of Mulla et al. [6], the Langmuir–Hinshelwood mechanism was proposed for NO oxidation on Pt/Al_2O_3 and the adsorption of O_2 on Pt sites ($O_2 + Pt \rightarrow Pt–O_2$) was recognized as the rate-determining step. Although much work has been focused on platinum catalysts for NO oxidation, no general agreements are reached on the reaction mechanism. Pt/Al_2O_3 is studied as a model catalyst for NO oxidation, while other platinum catalysts, *e.g.* Pt/TiO_2, receive much less attention.

The deactivation by SO_2 poisoning is a serious problem during the application of platinum catalysts for NO oxidation. According to the literature results [3,7], the NO oxidation activity over platinum catalysts (*e.g.* Pt/SiO_2 and Pt/Al_2O_3) dropped dramatically in the presence SO_2 at ppm level. The oxidation of SO_2 to SO_3 was reported to occur on the Pt sites of catalysts and the accumulation of surface sulfate was proposed as the main reason for SO_2 poisoning [3]. Apart from this, little information on the effects of SO_2 on NO oxidation is available. The detailed investigation on the mechanism of SO_2 poisoning is thus desired not only for the understanding of SO_2 poisoning during NO oxidation but also for the future design of SO_2-resistant NO oxidation catalysts.

In our previous work [8], we reported that Pt/TiO_2 catalyst prepared by photo-deposition exhibited remarkable activity for NO oxidation even in the presence of SO_2. In the present work, the surface species formed during the NO oxidation under different conditions (in the absence/presence of SO_2) over Pt/TiO_2 prepared by photo-deposition are investigated by in situ FTIR spectroscopy. The reaction pathways for NO oxidation over Pt/TiO_2 will be dis-

---

* Corresponding author at: Research Center for Eco-Environmental Sciences, Chinese Academy of Sciences, 18 Shuangqing Road, Haidian District, Beijing 100085, PR China. Tel.: +86 10 62923564; fax: +86 10 62923564.
E-mail address: zpinghao@rcees.ac.cn (Z. Hao).

0920-5861/$ – see front matter © 2010 Elsevier B.V. All rights reserved.
doi:10.1016/j.cattod.2010.04.038

cussed based on the results and the effects of SO_2 on NO oxidation will be proposed.

2. Experimental

2.1. Preparation of Pt/TiO$_2$ catalyst

The detailed preparation process of Pt/TiO_2 by photo-deposition can be found in our previous work [8]. Briefly, 2 mM H_2PtCl_6 solution containing *ca.* 0.01 g Pt, 500 mg of TiO_2 and 8 mL of ethanol were added into a round-bottom quartz flask under stirring to form slurry. The slurry was adjusted to pH 10.5 ± 0.5 and irradiated by a high-pressure mercury light for 6 h. Finally, the particles were filtered, washed, and dried at ambient conditions.

2.2. Catalytic oxidation of nitric oxide

The catalytic oxidation of NO was performed in a fixed-bed flow microreactor at atmospheric pressure. Typically, 0.15 g sample (sieve fraction of 0.16–0.25 mm) was placed in a quartz reactor (4 mm i.d.) and pretreated in 5%O_2/He at 450 °C for 1 h. After cooling to 150 °C in He, the reactant gas mixture (400 ppm NO, 0 ppm or 320 ppm SO_2, 10% O_2, He balance) was fed to the reactor. The total flow rate of the gas mixture was kept at 450 mL min^{-1}, corresponding to a GHSV of 180,000 h^{-1}. The inlet and outlet gases were monitored on-line using a gas chromatograph (HP 6820 series, for N_2 and N_2O analysis) and a chemiluminescence NO*x* analyzer (Ecotech EC 9841, for NO and NO_2 analysis).

2.3. In situ FTIR study on NO oxidation

In situ FTIR studies were performed on the spectrometer (Bruker Tensor 27) by using a diffuse reflectance attachment (HARRICK) equipped with a reaction chamber. 128 single beam spectra had been co-added at a resolution of 4 cm^{-1} and the spectra were presented as Kubelka–Munk function referred to adequate background spectra. The samples were used as self-supporting wafers (*ca.* 20 mg) and pretreated in 5%O_2/He at 450 °C for 1 h prior to adsorption experiments. After cooling to desired temperature in flowing He, the samples were exposed to certain reactant gas mixture at a constant temperature and time-resolved FTIR spectra were recorded. To obtain the temperature-resolved FTIR spectra, the sample in flowing gas stream was adjusted to a desired temperature and spectra were recorded after 20 min steady-state reaction at this temperature.

2.4. Thermal decomposition of surface nitrates

The thermal decomposition of surface nitrates on Pt/TiO_2 catalyst was performed on a fixed-bed flow reactor with a quartz tube. Pt/TiO_2 sample of 0.5 g (sieve fraction of 0.16–0.25 mm) was fixed in the tube and pretreated with flowing 5%O_2/He at 450 °C for 1 h and then cooled down to 150 °C in flowing He. A mixture of 400 ppm NO, 0 ppm or 320 ppm SO_2, 10% O_2, and the balance He was introduced to the sample at the constant temperature of 150 °C for 30 min. After NO–O_2 steady-state adsorption, the sample was purged with He at 150 °C for 30 min to remove the physisorbed NO or NO_2. Finally, the temperature-programmed decomposition of surface nitrates was conducted from 150 °C to 550 °C (no decomposition product can be found at above 550 °C) with a heating-rate of 5 °C min^{-1} in He flow of 100 mL min^{-1}. The outlet NO and NO_2 were monitored on-line with a chemiluminescence NO*x* analyzer (Ecotech EC 9841).

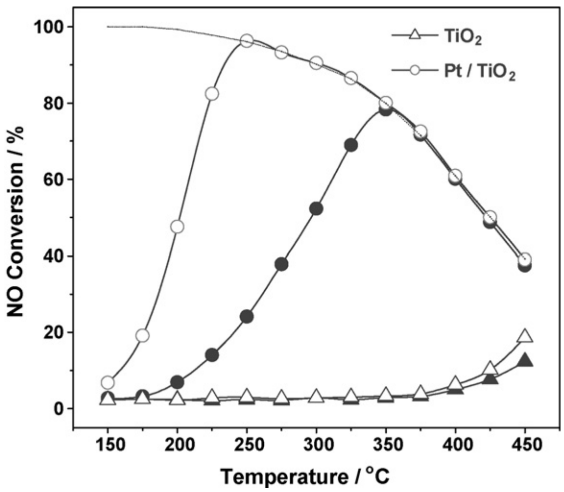

Fig. 1. NO oxidation on TiO_2 and Pt/TiO_2. Reaction conditions: 0.15 g catalyst, 400 ppm NO, 0 ppm (empty symbol) or 320 ppm (filled symbol) SO_2, 10% O_2, He balance, GHSV = 180,000 h^{-1}.

3. Results and discussion

3.1. Catalytic activity for NO oxidation on Pt/TiO$_2$

The catalytic activity for NO oxidation on TiO_2 and Pt/TiO_2 is shown in Fig. 1. TiO_2 support exhibits quite low activity (<20%) for NO oxidation both in the presence of SO_2 and in the absence of SO_2, suggesting that the high NO oxidation activity of Pt/TiO_2 is originated from Pt.

In the absence of SO_2, a 50% NO conversion to NO_2 is achieved at *ca.* 210 °C on Pt/TiO_2 and a maximal NO conversion of *ca.* 94% is achieved at 250 °C. Above 250 °C, the NO conversion decreases along the thermodynamic equilibrium of NO–NO_2 (the dash line in the figure). While in the presence of SO_2, a maximal NO conversion of *ca.* 75% is achieved at 350 °C on Pt/TiO_2 and NO conversion then decreases along the thermodynamic equilibrium at above 350 °C. It is seen that SO_2 shows obvious negative effect on NO oxidation. Nevertheless, considerable NO oxidation activity is achieved on Pt/TiO_2 with SO_2 in the stream and to our knowledge, Pt/TiO_2 is the most active catalyst for NO oxidation in the presence of high concentration SO_2.

3.2. NO adsorption and NO–O$_2$ co-adsorption at room temperature

Introduction of 400 ppm NO to Pt/TiO_2 at room temperature results in the appearance of several IR bands corresponding to different surface species, as displayed in Fig. 2A. After 3 min of adsorption, bands at 1600 cm^{-1}, 1585 cm^{-1}, 1480 cm^{-1}, 1300 cm^{-1} and 1260 cm^{-1}, together with a band at 1785 cm^{-1} are observed. The bands at 1300 cm^{-1} and 1585 cm^{-1} are assigned to chelating bidentate nitrates on TiO_2, while the bands at 1600 cm^{-1} and 1260 cm^{-1} are assigned to bridging bidentate nitrates on TiO_2 [9,10]. The band at 1480 cm^{-1} is assigned to monodentate nitrates on TiO_2 surface [11] and the band at 1785 cm^{-1} is assigned to linear NO species on Pt particles [12,13]. With increasing adsorption time, the intensities of IR bands corresponding to nitrates on TiO_2 increase, while the intensity of IR band corresponding to linear NO species on Pt remains almost unchanged. During the NO adsorption process at room temperature, predominant nitrates are formed on TiO_2 support. In our opinion, NO initially adsorbs on Pt sites as linear NO species, which are further oxidized and migrate to TiO_2 support to form various surface nitrates. For reference, the spectra of NO adsorption on TiO_2 support (Degussa P25) at room tempera-

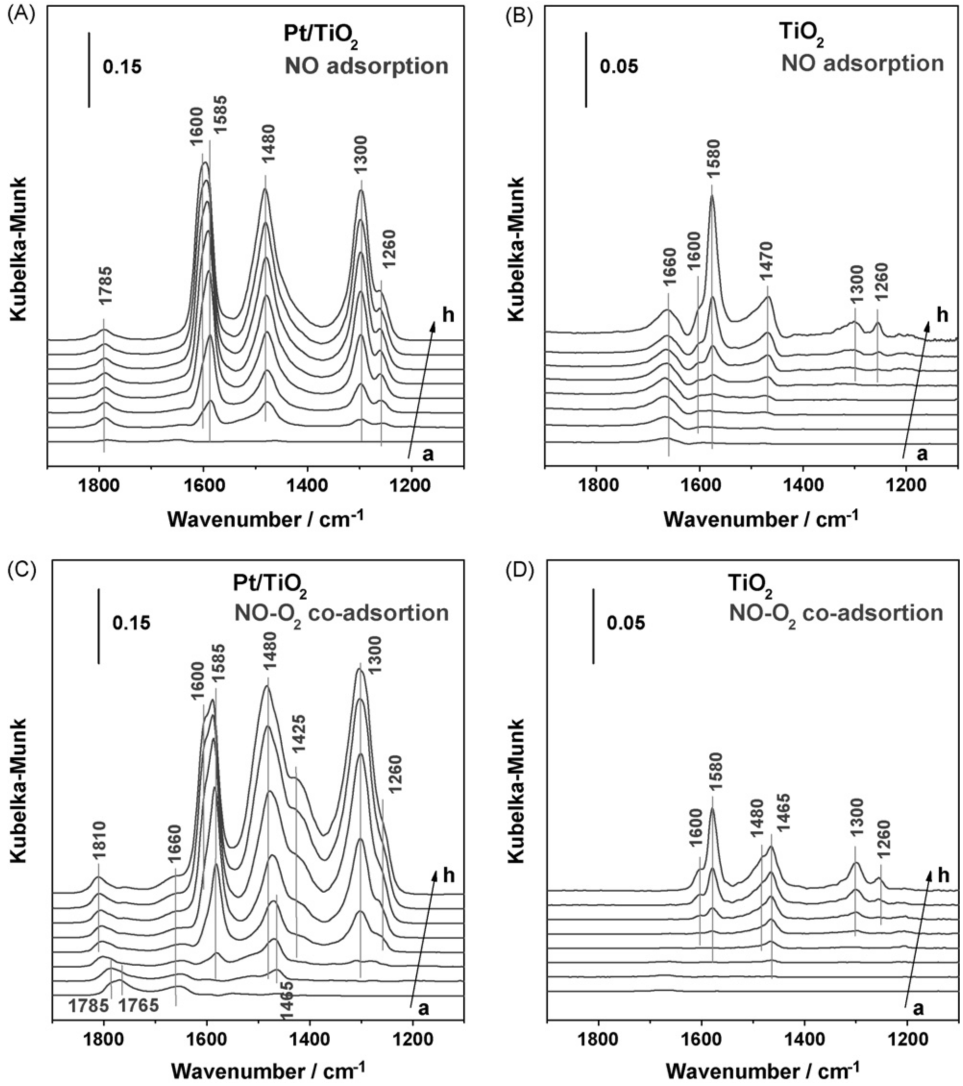

Fig. 2. In situ FTIR spectra of surface species on Pt/TiO_2 and TiO_2 during NO adsorption (400 ppm NO, He balance) and NO–O_2 co-adsorption (400 ppm NO–10% O_2, He balance) at room temperature for 1 min (a), 3 min (b), 5 min (c), 7 min (d), 9 min (e), 11 min (f), 13 min (g) and 15 min (h).

ture are shown in Fig. 2B and various nitrates (bands at 1600 cm^{-1}, 1580 cm^{-1}, 1470 cm^{-1}, 1300 cm^{-1} and 1260 cm^{-1}), together with adsorbed N_2O_3 [14] (tentative assignment, bands at 1660 cm^{-1}), are observed on the surface of TiO_2. The nitrates species are directly formed on the surface of TiO_2 and the intensities of IR bands associated with nitrates species are much lower compared to those on Pt/TiO_2 (note the different *y* axis scales).

FTIR spectra during exposure of Pt/TiO_2 to NO–O_2 at room temperature are shown in Fig. 2C. FTIR bands at 1785 cm^{-1}, 1765 cm^{-1}, 1660 cm^{-1} and 1465 cm^{-1} are observed on sample upon NO–O_2 co-adsorption. The bands at 1785 cm^{-1} and 1765 cm^{-1} are assigned to linear NO species on different Pt sites [13,15]. It is seen that NO mainly adsorbs as linear NO on Pt sites at the beginning of adsorption. With increasing adsorption time, the linear NO species are gradually oxidized to monodentate nitrites, as illustrated by the band at 1465 cm^{-1} [16]. The adsorbed N_2O_3 species may be the intermediates of this process. The monodentate nitrites can transform to nitro compound (band at 1425 cm^{-1} [17]) or further oxidized to various nitrates (bands at 1600 cm^{-1}, 1585 cm^{-1}, 1480 cm^{-1}, 1300 cm^{-1} and 1260 cm^{-1}). During the adsorption process, the linear NO species on Pt gradually transform to NO dimers on Pt, as illustrated by the band at 1810 cm^{-1} [17]. Generally, NO dimers are not stable species on Pt sites. While in this work, the NO dimers are stabilized on Pt site by π-back donation, originated from the interaction between Pt and O. On the whole, NO initially adsorbs Pt sites as linear NO species in excess oxygen and the linear NO species are finally oxidized to surface nitrates on TiO_2 through certain intermediates at room temperature. In the spectra of NO–O_2 co-adsorption on TiO_2 (Fig. 2D), various surface nitrates (bands at 1660 cm^{-1}, 1600 cm^{-1}, 1580 cm^{-1}, 1470 cm^{-1}, 1300 cm^{-1} and 1260 cm^{-1}) are observed and their intensities develop with increasing adsorption time.

Based on the spectra of NO and NO–O_2 adsorption on TiO_2 and Pt/TiO_2, we observe that the introduction of Pt to TiO_2 by photo-deposition changes the formation of surface species during adsorption process at room temperature. It is also proposed that the addition of Pt greatly improves the oxidation activity of TiO_2, which promotes the formation surface nitrates.

3.3. NO–O_2, SO_2–O_2 and NO–SO_2–O_2 co-adsorption at different temperatures

In situ FTIR spectra obtained under steady-state reaction conditions over Pt/TiO_2 at different temperatures are shown in Fig. 3A. In flowing NO–O_2 at 175 °C, IR bands at 1810 cm^{-1}, 1650 cm^{-1}, 1610 cm^{-1}, 1585 cm^{-1}, 1515 cm^{-1}, 1350 cm^{-1}, 1290 cm^{-1} and

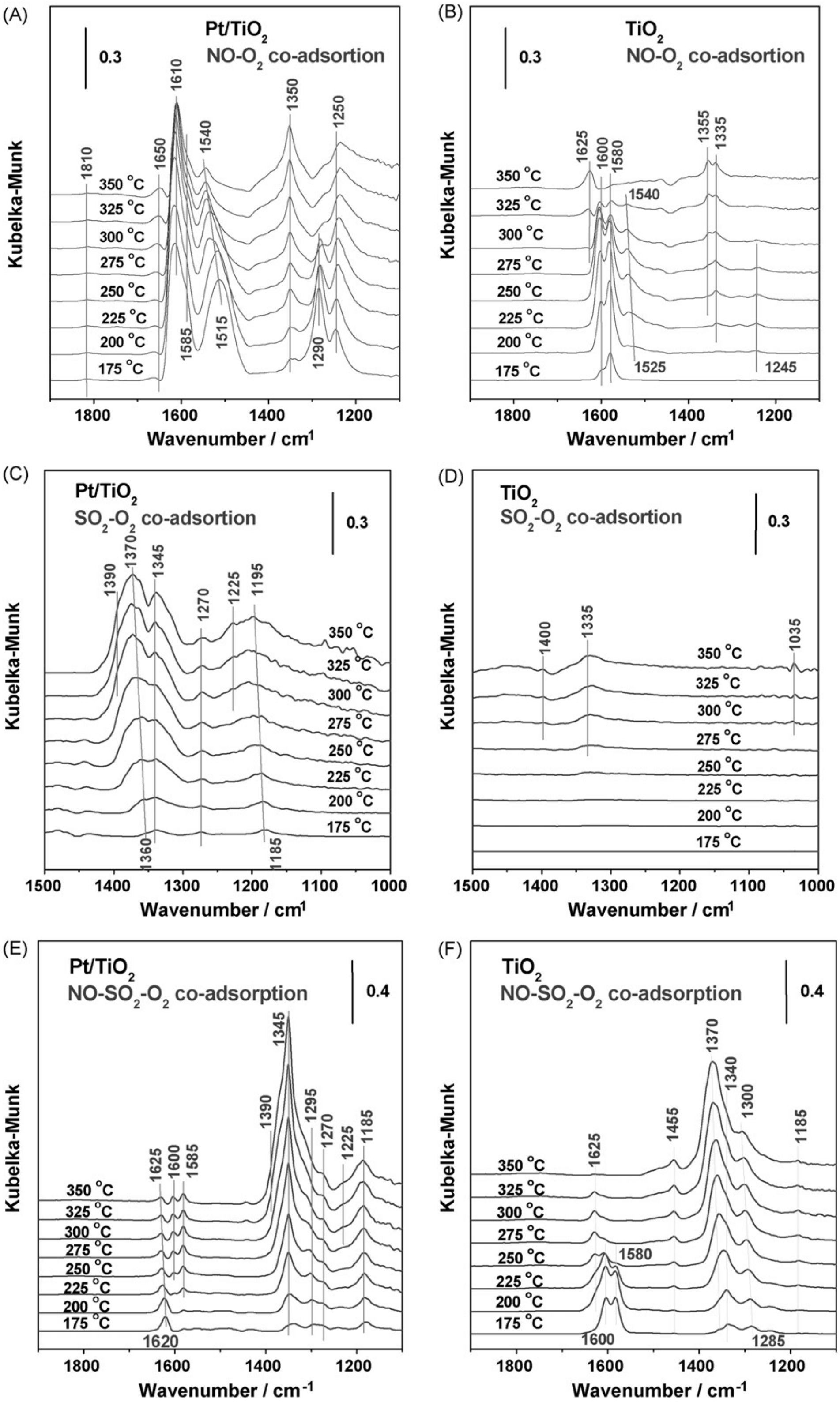

Fig. 3. In situ FTIR spectra of surface species on Pt/TiO_2 and TiO_2 during NO–O_2 co-adsorption (400 ppm NO–10% O_2, He balance), SO_2–O_2 co-adsorption (320 ppm SO_2–10% O_2, He balance) and NO–SO_2–O_2 co-adsorption (400 ppm NO–320 ppm SO_2–10% O_2, He balance) at different temperatures.

1250 cm^{-1} are observed. The bands at 1610 cm^{-1} and 1250 cm^{-1} are assigned to bridging bidentate nitrates, while the bands at 1585 cm^{-1} and 1290 cm^{-1} are assigned to chelating bidentate nitrates. These bands shift to higher or lower frequencies compared to those formed at room temperature (ref. Fig. 2C). The strong broad band at 1515 cm^{-1} is assigned to monodentate nitrates and the weak band at 1350 cm^{-1} is assigned to free nitrates [16]. The band at 1810 cm^{-1} corresponding to adsorbed NO dimers on Pt is very weak and is hardly to distinguish. Under steady-state NO–O_2 reaction at 175 °C, the main surface species formed on Pt/TiO_2 catalyst

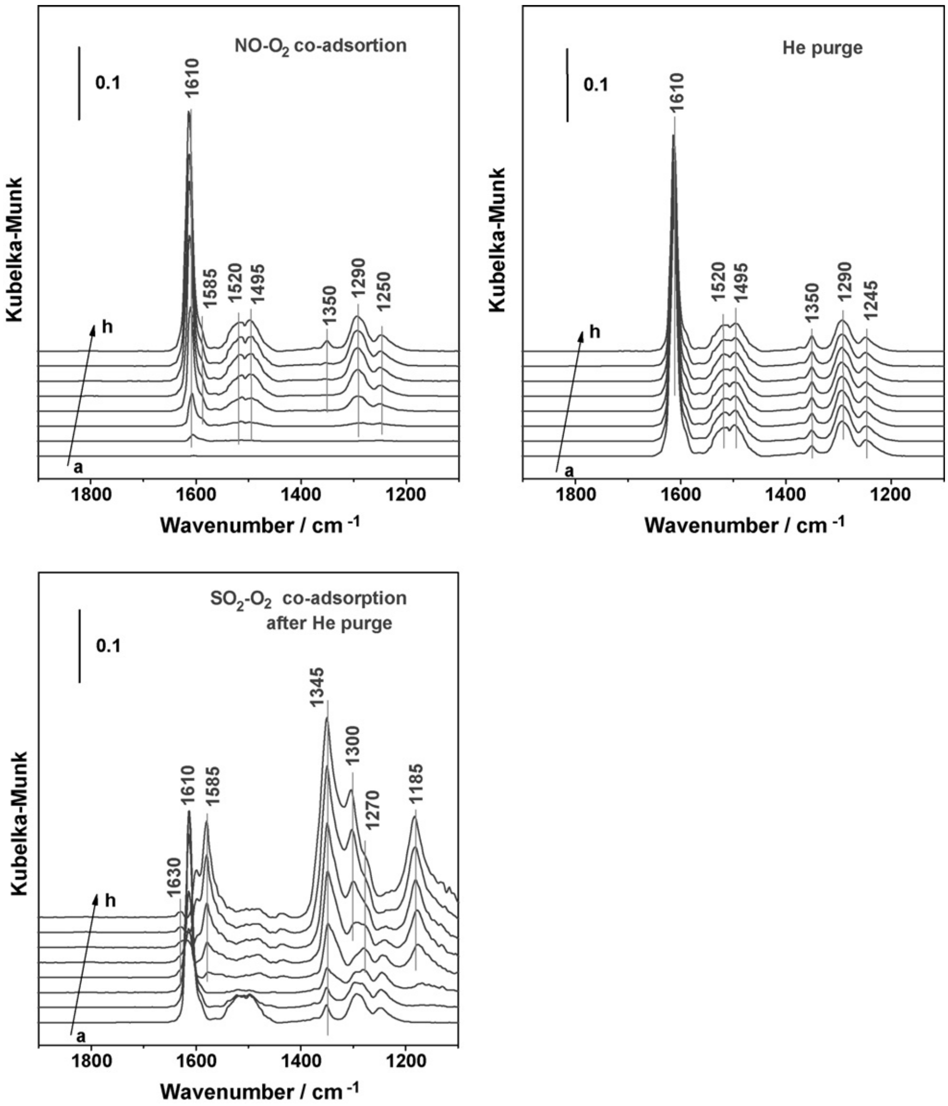

Fig. 4. In situ FTIR spectra of surface species on Pt/TiO_2 during NO–O_2 co-adsorption (400 ppm NO–10% O_2, He balance), subsequent He purge and SO_2–O_2 co-adsorption (320 ppm SO_2–10% O_2, He balance) at 250 °C for 1 min (a), 3 min (b), 5 min (c), 7 min (d), 9 min (e), 11 min (f), 13 min (g) and 15 min (h).

are various nitrates associated with TiO_2. With increasing reaction temperature from 175 °C to 350 °C, the intensities of IR bands corresponding to chelating bidentate nitrates gradually decrease, while the intensities of IR bands corresponding to free nitrates increase. As for IR bands corresponding to bridging bidentate nitrates, the intensities first increase to the maximum (at *ca.* 250 °C) and then begin to decrease. Besides, the monodentate nitrates at 1515 cm^{-1} sharply decrease with increasing temperature and shift to higher frequencies (at 1540 cm^{-1} at 350 °C). Based on the changes of IR bands corresponding to various nitrates at different temperatures, the stability of surface nitrates are distinguished as monodentate nitrates < chelating bidentate nitrates < bridging bidentate nitrates < free nitrates, basically in consistent with the literature results [18]. In the spectra of NO–O_2 adsorption on TiO_2 at different temperatures (Fig. 3B), the transformation of different surface nitrates are also observed and the corresponding stability of surface nitrates are distinguished as the same order.

In flowing SO_2–O_2 at 175 °C, IR bands at 1360 cm^{-1}, 1345 cm^{-1}, 1270 cm^{-1} and 1185 cm^{-1} are observed on Pt/TiO_2, as shown in Fig. 3C. The bands at 1360 cm^{-1} and 1185 cm^{-1} are assigned to gas-phase or so-called physisorbed (non-chemisorbed) SO_2 [19], while the band at 1345 cm^{-1} and 1270 cm^{-1} are assigned to chemisorbed SO_2 [20,21]. Besides, no IR bands corresponding to sulfate species, *e.g.* bands at 1125 cm^{-1} and 1160 cm^{-1} [22], can be observed. It is seen that SO_2 is not oxidized on Pt/TiO_2 at 175 °C. With increasing reaction temperature from 175 °C to 275 °C, the intensities of IR bands corresponding to physisorbed SO_2 and chemisorbed SO_2 increase. Meanwhile, the IR bands corresponding to physisorbed SO_2 shift a little to higher frequencies. At *ca.* 300 °C, new IR bands at 1390 cm^{-1} and 1225 cm^{-1} appear. The band at 1225 cm^{-1} is assigned to adsorbed SO_3^- species [23] and the band at 1390 is assigned to physisorbed SO_3 [19]. It is thus deduced that SO_2 is oxidized to SO_3 at above 300 °C on Pt/TiO_2 catalyst via adsorbed SO_3^- as possible intermediate.

The surface species formed on TiO_2 during SO_2–O_2 adsorption differ greatly from those on Pt/TiO_2, as displayed in Fig. 3D. At below 250 °C, no obvious surface species are formed on the surface of TiO_2. At above 250 °C, weak IR bands at 1335 cm^{-1} and 1035 cm^{-1} corresponding to ν(S=O) and ν(S–O) of surface sulfates [24], together with very weak IR band at 1400 cm^{-1} corresponding to $S_2O_7^{2-}$ or SO_3 like species [25], are observed, indicating the oxidation of SO_2. From these results, it is seen that TiO_2 support employed in this study is relatively SO_2-resistant and surface sulfates are not easily formed, in great contrast to other oxides, *e.g.* CeO_2 and Al_2O_3. From the spectra of SO_2–O_2 adsorption on Pt/TiO_2 and TiO_2 (Fig. 3C and D), we can conclude that the addition of Pt to TiO_2 significantly

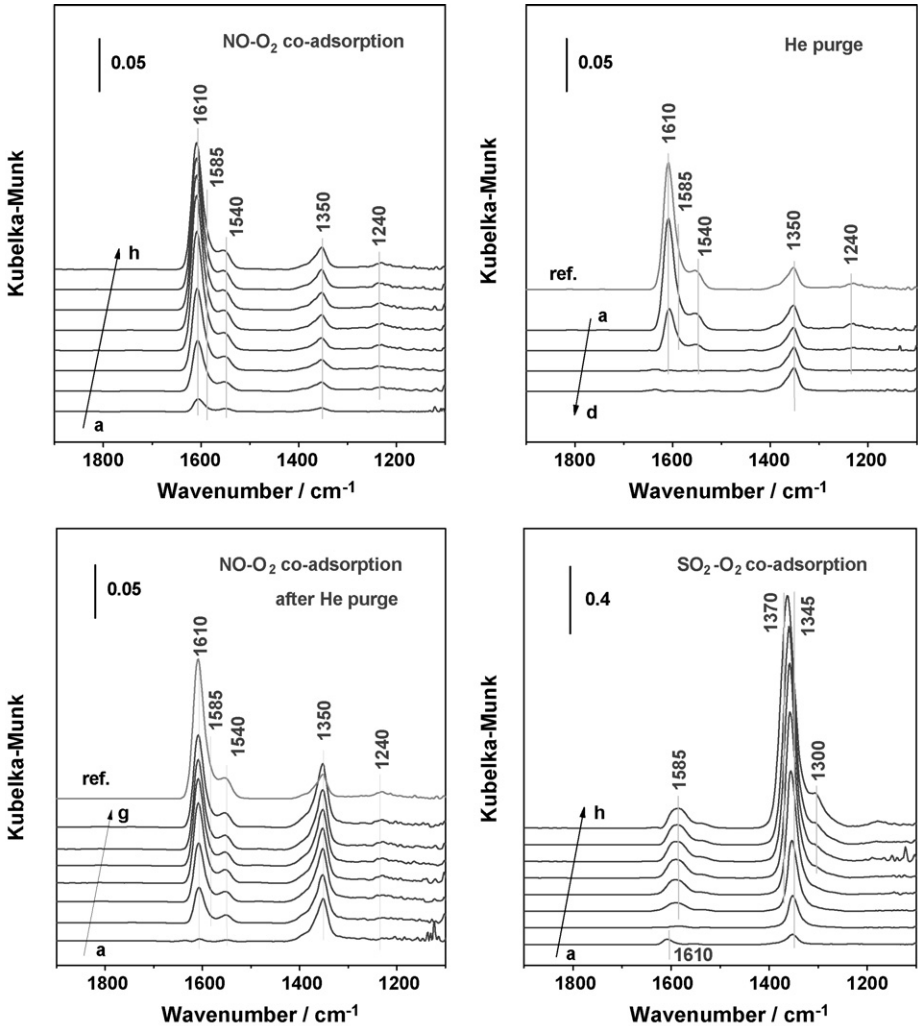

Fig. 5. In situ FTIR spectra of surface species on Pt/TiO_2 during $NO–O_2$ co-adsorption (400 ppm NO–10% O_2, He balance), subsequent He purge, $NO–O_2$ re-adsorption (400 ppm NO–10% O_2, He balance) and $SO_2–O_2$ co-adsorption (320 ppm SO_2–10% O_2, He balance) at 350 °C for 1 min (a), 3 min (b), 5 min (c), 7 min (d), 9 min (e), 11 min (f), 13 min (g) and 15 min (h).

promotes the adsorption (both physisorption and chemisorption) of SO_2.

When Pt/TiO_2 is exposed to the stream containing both NO and SO_2 ($NO–SO_2–O_2$/He), IR bands corresponding to surface nitrate species and chemisorbed SO_2 can be observed, as shown in Fig. 3E. At 175 °C, chemisorbed SO_2 (bands at 1345 cm^{-1} and 1270 cm^{-1}), bridging bidentate nitrates (band at 1620 cm^{-1}) and chelating bidentate nitrates (band at 1300 cm^{-1}) are observed. The intensities of IR bands corresponding to nitrate species in flowing $NO–SO_2–O_2$/He are much lower than those in $NO–O_2$/He, indicating that the addition of SO_2 greatly suppress the formation of nitrates species on catalyst. The monodentate nitrates (IR band at 1515 cm^{-1}) formed in flowing $NO–O_2$/He are no longer observed in flowing $NO–SO_2–O_2$/He. The free nitrates with IR band at 1350 cm^{-1}, even if exist, cannot be distinguished due to overlapping by the strong IR band at 1345 cm^{-1}. All these changes in surface nitrates, both in intensities and types, are ascribed to the occupation of adsorption sites of Pt/TiO_2 by SO_2. The intensities of IR bands corresponding to chemisorbed SO_2 increase with increasing reaction temperatures, while the intensities of surface nitrates do not show obvious changes. The oxidation of SO_2 to SO_3 is proved by the appearance of IR bands at 1225 cm^{-1} and 1390 cm^{-1} at above 300 °C.

In flowing $NO–SO_2–O_2$/He, the surface species formed on TiO_2 are shown in Fig. 3F. It is seen that surface nitrates (bands at 1600 cm^{-1} and 1580 cm^{-1}) are predominant species at lower temperatures, while they are gradually replaced by physisorbed SO_2 (bands at 1370 cm^{-1} and 1185 cm^{-1}) with increasing temperatures. The transformation of surface nitrates, from chelating nitrates (1580 cm^{-1}) to bridging nitrates (1600 cm^{-1}), is also observed. Based on the surface species formed on TiO_2 during $SO_2–O_2$ (Fig. 3D) and $NO–SO_2–O_2$ adsorption (Fig. 3F), we clearly observe that the existence of NO in the stream greatly promotes the physisorption of SO_2 on TiO_2.

Based on the results in Fig. 3, we conclude that the addition of Pt greatly changes the properties of TiO_2 and thus changes the surface species formed during adsorption. As for Pt/TiO_2, it is found that the existence of NO does not influence the adsorption of SO_2, while the existence of SO_2 greatly suppresses the formation of nitrates. The occupation of active sites by SO_2 adsorption without the formation of surface sulfates should be the key reason for Pt/TiO_2 deactivation by SO_2 at relative low temperatures.

3.4. Stability of surface nitrate species on Pt/TiO_2 at 250 °C

Time-resolved FTIR spectra of $NO–O_2$ co-adsorption on Pt/TiO_2 at 250 °C are shown in Fig. 4. The adsorbed species are attributed to various surface nitrates: bridging bidentate nitrates (IR bands at 1610 cm^{-1} and 1250 cm^{-1}), chelating bidentate nitrates (IR bands at 1585 cm^{-1} and 1290 cm^{-1}), monodentate nitrates (IR bands

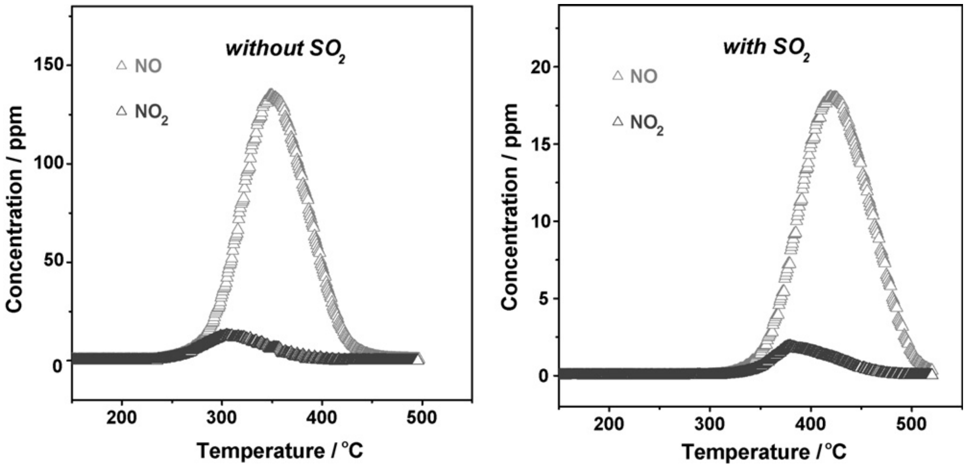

Fig. 6. Temperature-programmed decomposition of surface nitrates on Pt/TiO_2 after $NO–O_2$ co-adsorption at 150 °C.

at 1520 cm^{-1} and 1495 cm^{-1} [17]) and free nitrates (IR bands at 1350 cm^{-1}). After 15 min, the adsorption reach to saturation and the intensities of IR bands corresponding to various nitrates do not change any more.

After exposed in $NO–O_2/He$ for 15 min, the Pt/TiO_2 sample, with various nitrates on the surface, is purged in pure He at 250 °C for a period of time. It is easily seen that all IR bands remains unchanged during He purge, indicating that all nitrates species are stable at 250 °C in He. After He purge, the sample is then exposed to $SO_2–O_2/He$ for a period of time. The introduction of $SO_2–O_2$ results in the appearance of IR bands corresponding to chemisorbed SO_2 (band at 1345 cm^{-1}) and the band intensities increase with time. With the adsorption of SO_2, the intensities of IR bands corresponding to unstable monodentate nitrates (bands at 1520 cm^{-1} and 1495 cm^{-1}) decrease and the band completely disappears after 5 min. It is also observed that bridging bidentate nitrates on TiO_2 (bands at 1610 cm^{-1} and 1270 cm^{-1}) gradually transform to chelating bidentate nitrates on TiO_2 (bands at 1585 cm^{-1} and 1300 cm^{-1}) accompanied by the adsorption of SO_2. Generally, the bridging nitrates are more stable species than chelating nitrates and the transformation from bridging nitrates to chelating nitrates is not preferred. In this work, because SO_2 occupies the adsorption sites on TiO_2 during adsorption process, the bridging nitrates (one nitrate on two adsorption sites) are thus forced to transform to chelating nitrates (one nitrate on one adsorption site).

3.5. *Stability of surface nitrate species on Pt/TiO_2 at 350 °C*

The FTIR spectra during exposure of Pt/TiO_2 to $NO–O_2/He$ at 350 °C are shown in Fig. 5. Bridging bidentate nitrates (IR bands at 1610 cm^{-1} and 1240 cm^{-1}), chelating bidentate nitrates (IR bands at 1585 cm^{-1}), monodentate nitrates (IR bands at 1540 cm^{-1}) and free nitrates (IR bands at 1350 cm^{-1}) are observed during $NO–O_2$ co-adsorption. After exposure to $NO–O_2$ for 15 min (reach to adsorption saturation), the Pt/TiO_2 sample is purged in He at 350 °C. The intensities of IR bands corresponding bridging nitrates, chelating nitrates and monodentate nitrates decrease drastically and these bands completely disappear after He purge for 5 min. Meanwhile, the IR band corresponding to free nitrates remains nearly unchanged. It is thus concluded that free nitrates are stable at 350 °C, while other types of nitrates are not stable and they will decompose at 350 °C. The decomposition of nitrates on catalyst may progress in the following two pathways [26]:

$$4NO_3^- \rightarrow 4NO_2(g) + O_2(g) + 2O^{2-}$$

$$4NO_3^- \rightarrow 4NO(g) + 3O_2(g) + 2O^{2-}$$

After He purge, the sample is again exposed to $NO–O_2/He$ at 350 °C. It is seen that the former disappeared nitrates (bridging nitrates, chelating nitrate and monodentate nitrates) recover with the re-adsorption of $NO–O_2$. Moreover, the intensity of IR band corresponding to free nitrates after re-adsorption of $NO–O_2$ becomes much higher than that after initial $NO–O_2$ adsorption (indicated as ref. in Fig. 5).

After the re-adsorption of $NO–O_2$, the Pt/TiO_2 sample is finally exposed to $SO_2–O_2/He$. With the introduction of $SO_2–O_2$, the IR bands corresponding to physisorbed SO_2 at 1370 cm^{-1} and chemisorbed SO_2 at 1350 cm^{-1} appear. Meanwhile, the bridging bidentate nitrates (IR bands at 1610 cm^{-1}) gradually transform to chelating bidentate nitrates (IR bands at 1785 cm^{-1} and 1300 cm^{-1}), similar to that happens at 250 °C. Any changes on IR band at 1350 cm^{-1} corresponding to free nitrates are hardly observed due to the overlap of strong bands at 1345 cm^{-1} corresponding to chemisorbed SO_2.

3.6. *Temperature-programmed decomposition of surface nitrates*

The temperature-programmed decomposition profiles of surface nitrates on Pt/TiO_2 after $NO–O_2$ adsorption are presented in Fig. 6. It is seen that the surface nitrates begin to decompose at *ca.* 250 °C when SO_2 is absent during adsorption, indicating the chemisorbed nitrates are stable up to 250 °C. It is also seen that the main products from nitrates decomposition is NO and only a very small quantity of NO_2 is detected at the beginning of nitrates decomposition. When SO_2 is present during adsorption, the decomposition temperature of surface nitrates is put off to *ca.* 350 °C. The improved stability of surface nitrate is ascribed to the effects of SO_2 on nitrates formation. As discussed in Section 3.3, the SO_2 in reaction stream may suppress the formation of surface nitrates, especially the most unstable monodentate nitrates. As a result, the decomposition of nitrates is retarded to higher temperatures. Moreover, the amount of NO detected in the decomposition products is much less than that without SO_2 during $NO–O_2$ adsorption.

3.7. *NO oxidation pathways on Pt/TiO_2*

The NO oxidation pathways on Pt/TiO_2 are proposed based on the results obtained, as illustrated in Fig. 7. In the first step, oxygen adsorbs on the surface of Pt, followed by the disassociation to O [27]:

$$Pt + O_2(g) \rightarrow Pt–O_2 \qquad (R1)$$

$$Pt–O_2 + Pt \rightarrow 2Pt–O \qquad (R2)$$

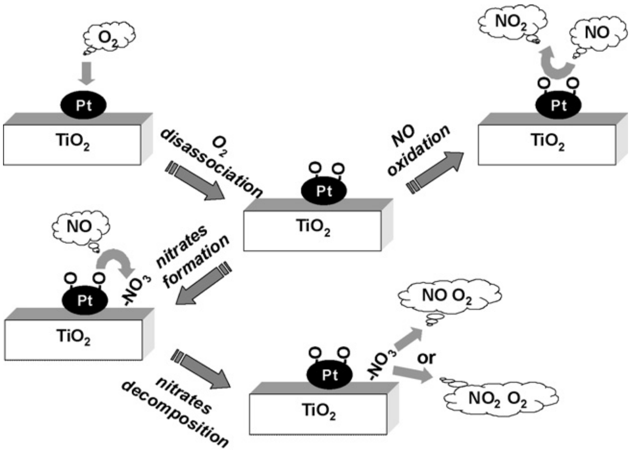

Fig. 7. Proposed NO oxidation pathways on Pt/TiO_2 catalysts.

Gaseous NO can react with surface oxygen to form gaseous NO_2:

$$Pt\text{–}O + NO(g) \rightarrow Pt + NO_2(g) \tag{R3}$$

Gaseous NO can also react with surface oxygen to form nitrates, which then migrate to adsorption sites of TiO_2 support, similar to a NO storage process [28]:

$$3Pt\text{–}O + 2NO(g) + O^{2-} \rightarrow 3Pt + 2NO_3^{-} \tag{R4}$$

At relative high temperatures, the formed nitrates may decompose to produce gaseous NO or NO_2:

$$4NO_3^{-} \rightarrow 4NO_2(g) + O_2(g) + 2O^{2-} \tag{R5}$$

$$4NO_3^{-} \rightarrow 4NO(g) + 3O_2(g) + 2O^{2-} \tag{R6}$$

From the FTIR spectra of NO–O_2 co-adsorption in Fig. 2, it is seen that NO can be oxidized by surface oxygen to form surface nitrates even at room temperature (R4). From the catalytic results, gaseous product NO_2 cannot be detected until 150 °C, suggesting that the direct oxidation of gaseous NO to NO_2 (R3) does not take place at below 150 °C. The surface nitrates species are stable up to 250 °C and the decomposition of surface nitrates does not take place at below 250 °C. So, the reactions under our experimental conditions at below 150 °C are (R1), (R2) and (R4) In the temperature range of 150–250 °C, NO_2 is detected in the product due to the direct oxidation of gaseous NO (R3) and the decomposition of surface nitrates still does not take place. So, the reactions at 150–250 °C are (R1–R4). It should be noted that reaction (R4) will be suspended once the adsorption of nitrates reaches to saturation at below 250 °C. At above 250 °C, on one side, surface nitrates decompose to NO (a very small proportion to NO_2) and on the other side gaseous NO is oxidized to gaseous NO_2 or adsorbed nitrates. So, the reactions at above 250 °C include (R1–R6). Based on the thermodynamic balance between NO and NO_2, the NO conversion to NO_2 gradually drops along the thermodynamic equilibrium.

As discussed above, the direct oxidation of gaseous NO is the only pathway for NO_2 formation on Pt/TiO_2 catalysts at 150–250 °C and it is still the main pathway for NO_2 formation at above 250 °C. It can also be concluded that gaseous NO prefers to react with surface oxygen to form nitrates (R4) rather than to form gaseous NO_2 (R3) considering the different temperatures required for the two reactions. When SO_2 is added into the reaction stream, the formation of surface nitrates is greatly suppressed and thus the direct oxidation of gaseous NO may be accelerated. However, SO_2 may also block most available Pt sites and as an integrated result, the existence of SO_2 in reaction stream shows negative effect on NO oxidation to some extent.

4. Conclusion

The main surface species formed during the exposure of Pt/TiO_2 to NO–O_2 at different temperatures are various types of nitrates. Exposure of catalyst to SO_2–O_2 results in the formation of adsorbed SO_2 on surface and the oxidation of SO_2 to SO_3 is observed only at above 300 °C. When Pt/TiO_2 is exposed to a gas mixture containing NO–SO_2–O_2, both surface nitrates and adsorbed SO_2 are observed. The existence of NO does not influence the adsorption and oxidation of SO_2, while the existence of SO_2 greatly suppresses the formation of surface nitrates and changes the types of nitrates formed as well.

The thermal decomposition of surface nitrates on Pt/TiO_2 occurs at elevated temperature and the main decomposition product is NO. The existence of SO_2 during NO–O_2 adsorption retards the decomposition of nitrates because SO_2 prohibits the formation of unstable surface nitrates.

The direct oxidation of gaseous NO is the only pathway for NO_2 formation on Pt/TiO_2 catalyst at temperatures below the decomposition of surface nitrates and it is still the main pathway for NO_2 formation at temperatures above the decomposition of surface nitrates. The decomposition of surface nitrates plays an obvious negative role for NO oxidation because the main decomposition product is NO instead of NO_2.

Acknowledgement

This work was financially supported by the National Natural Science Foundation of China (20703057 and 20725723).

References

[1] Z.M. Liu, S.I. Woo, Recent advances in catalytic DeNO*x* science and technology, Catal. Rev. Sci. Eng. 48 (2006) 43–89.
[2] W.S. Epling, L.E. Campbell, A. Yezerets, N.W. Currier, J.E. Parks II, Overview of the fundamental reactions and degradation mechanisms of NO*x* storage/reduction catalysts, Catal. Rev. Sci. Eng. 46 (2004) 163–245.
[3] E. Xue, K. Seshan, J.R.H. Ross, Roles of supports, Pt loading and Pt dispersion in the oxidation of NO to NO_2 and of SO_2 to SO_3, Appl. Catal. B 11 (1996) 65–79.
[4] L. Olsson, B. Westerberg, H. Persson, E. Fridell, M. Skoglundh, B. Andersson, A kinetic study of oxygen adsorption/desorption and NO oxidation over Pt/Al_2O_3 catalysts, J. Phys. Chem. B 103 (1999) 10433–10439.
[5] L. Olsson, H. Persson, B.E. Fridell, M. Skoglundh, B. Andersson, A kinetic study of NO oxidation and NO*x* storage on Pt/Al_2O_3 and Pt/BaO/Al_2O_3, J. Phys. Chem. B 105 (2001) 6895–6906.
[6] S.S. Mulla, N. Chen, L. Cumaranatunge, G.E. Blau, D.Y. Zemlyanov, W.N. Delgass, S. Epling, F.H. Ribeiro, Reaction of NO and O_2 to NO_2 on Pt: kinetics and catalyst deactivation, J. Catal. 241 (2006) 389–399.
[7] Y.Y. Ji, T.J. Hoops, U.M. Graham, G. Jacobs, M. Crocker, A kinetic and DRIFTS study of supported Pt catalysts for NO oxidation, Catal. Lett. 110 (2006) 29–37.
[8] L.D. Li, Q. Shen, J. Cheng, Z.P. Hao, Catalytic oxidation of NO over TiO_2 supported platinum clusters. I. Preparation, characterization and catalytic properties, Appl. Catal. B 93 (2010) 259–266.
[9] M.A. Debeila, N.J. Coville, M.S. Scurrell, G.R. Hearne, The effect of calcination temperature on the adsorption of nitric oxide on Au–TiO_2 drifts studies, Appl. Catal. A 291 (2005) 98–115.
[10] K. Hadjiivanov, H. Knozinger, Species formed after NO adsorption and NO + O_2 coadsorption on TiO_2, Phys. Chem. Chem. Phys. 2 (2000) 2803–2806.
[11] M. Kantcheva, Identification, stability, and reactivity of NO*x* species adsorbed on titania-supported manganese catalysts, J. Catal. 204 (2001) 479–494.
[12] N.P. Magtoto, N.L. Sefara, H.H. Richardson, Two-dimensional FT-IR correlation analysis of the chemisorption of nitric oxide on Pt(1 0 0), Appl. Spectrosc. 53 (1999) 178–183.
[13] B.A. Morrow, R.A. McFarlane, L.E. Moran, Infrared study of the reaction between nitric oxide and molecular oxygen and of the adsorption of nitrogen dioxide on platinum, J. Phys. Chem. 89 (1985) 77–80.
[14] T. Ohno, F. Hatayama, Y. Toda, S. Konishi, H. Miyata, Fourier transform infrared studies of reduction of nitric oxide by ethylene over V_2O_5 layered on ZrO_2, Appl. Catal. B 5 (1994) 89–101.
[15] A. Bourane, O. Dulaurent, S. Salasc, C. Sarda, C. Bouly, D. Bianchi, Heats of adsorption of linear NO species on a Pt/Al_2O_3 catalyst using in situ Infrared spectroscopy under adsorption equilibrium, J. Catal. 204 (2001) 77–88.
[16] K. Hadjiivanov, V. Bushev, M. Kantcheva, D. Klissurski, Infrared spectroscopy study of the species arising during nitrogen dioxide adsorption on titania (anatase), Langmuir 10 (1994) 464–471.

[17] K. Hadjiivanov, Identification of neutral and charged *NxOy* surface species by IR spectroscopy, Catal. Rev. Sci. Eng. 42 (2000) 71–144.

[18] G. Ramis, G. Busca, V. Lorenzelli, P. Forzatti, Fourier transform infrared study of the adsorption and coadsorption of nitric oxide, nitrogen dioxide and ammonia on TiO_2 anatase, Appl. Catal. 64 (1990) 243–257.

[19] T. Luo, J.M. Vohs, R.J. Gorte, An examination of sulfur poisoning on Pd/Ceria catalysts, J. Catal. 210 (2002) 397–404.

[20] S. Kataoka, E. Lee, M.I. Tejedor-Tejedor, M.A. Anderson, Photocatalytic degradation of hydrogen sulfide and in situ FT-IR analysis of reaction products on surface of TiO_2, Appl. Catal. B 61 (2005) 159–163.

[21] C. Quijada, A. Rodes, J.L. Vazquez, J.M. Perez, A. Aldaza, Electrochemical-behavior of aqueous SO_2 at electrodes in acidic medium – a voltammetric and in-situ Fourier-transform IR study. 1. Oxidation of SO_2 on Pt electrodes with sulfur–oxygen adsorbed species, J. Electroanal. Chem. 394 (1995) 217–227.

[22] K. Nakamoto, Infrared and Raman Spectra of Inorganic and Coordination Compounds, John Wiley, New York, 1997.

[23] D. Forney, C.B. Kellogg, W.E. Thompson, M.E. Jacox, The vibrational spectra of molecular ions isolated in solid neon. XVI. SO_2^+, SO_2^-, and $(SO_2)_2^-$, J. Chem. Phys. 113 (2000) 86–97.

[24] O. Saur, M. Bensitel, A.B.M. Saad, J.C. Lavalley, C.P. Tripp, B.A. Morrow, The structure and stability of sulfated alumina and titania, J. Catal. 99 (1986) 104–110.

[25] M. Waqif, P. Bazin, O. Saur, J.C. Lavalley, G. Blanchard, O. Touret, Study of ceria sulfation, Appl. Catal. B 11 (1997) 193–215.

[26] Z. Liu, J.A. Anderson, Influence of reductant on the thermal stability of stored NO*x* in Pt/Ba/Al_2O_3 NO*x* storage and reduction traps, J. Catal. 224 (2004) 18–27.

[27] G. Zhou, T. Luo, R.J. Gorte, An investigation of NO*x* storage on Pt–BaO–Al_2O_3, Appl. Catal. B 64 (2006) 88–95.

[28] L.D. Li, J.J. Yu, Z.P. Hao, Z.P. Xu, Novel Ru–Mg–Al–O catalysts derived from hydrotalcite-like compound for NO storage/decomposition/reduction, J. Phys. Chem. C 111 (2007) 10552–10559.